Investigation of slag weight fraction on mechanical, thermal and tribological properties of friction materials

Priyank Lohiya[1]
[1] Phd scholar, Mechanical engineering department, UIT-RGPV, Bhopal

Abstract

This paper aimed to investigation of blast furnace slags on mechanical, thermal and tribological properties of friction materials elaborated by the dry heat-press molding method. Physical, mechanical and thermal proper-ties were analyzed and tribological behavior was studied for varying the extent of doping (20–45 wt.%). The results indicate that the hardness decreases from 60.6 HRL to 55.0 HRL with increasing slag content from 0 to 45 wt.% But density is opposite for the doped samples. The impact strength gradually increases from 4.39 kJ/m^2 to 4.80 kJ/m^2 when the content of slag increases from 0 to 45 wt.%. Doping was also found to increase the friction coefficients but decrease wear rates, mass-loss and heat release. The sample S_4 has a more superior and stable friction coefficient than others because of the transfer layers formed on the surface of friction materials.

1. Introduction

Friction materials are widely used for brake systems in cars, trains, planes and other similar transports. With the rapid development of the automotive industry and an increase in the observance of environment issues, the use of high quality friction materials is becoming more and more important. Manufacturers rely on these materials exhibiting suitable and stable friction coefficient, excellent wear-resistant properties, sufficient mechanical strength, desirable physical properties, limited the braking noises, low costs and a low wear rates at various operating speeds, pressures, temperatures and environmental conditions [1–2]. But serious thermal fade often occurs in systems using traditional friction materials, meaning that the high-speeds and heavy loads gradually become too much for these systems to handle. As asbestos friction materials, there is a performance decline to happen for it under the high temperature. Asbestos is also extremely harmful to people's health and the environment, and thus has been banned in the majority of the world's countries [3]. Therefore, researchers have struggled to come up with an equally efficient and safer substitute. Fei et al.[4] added carbon fibers with different length to reinforce four friction materials. The authors found that the wear rate of the sample with 100 μm fibers was only 1.40×10^{-5} mm^3/J. Wang et al. [5] modified basalt fabric phenolic composites with graphite and nano-SiO_2. The authors showed that graphite was more beneficial than nano-SiO_2 in improving the tribological properties of basalt fabric composites when they were singly incorporated. The friction and wear behavior of the filled composites was improved further when

Published By:
International Journal of Engineering
Research in Current Trends

nano-SiO_2 and graphite were added together. Matějka et al. [6] studied silicon carbide abrasive of various particle sizes (40, 10, and 3 mm) enhance friction composites. The authors found that highest values of friction coefficient as well as the lowest fade for the composites containing the finest SiC fraction (median value 3 mm) were obtained. As we can see, different reinforced materials were used in these researches, and good friction and wear properties have been achieved. However, the price of these reinforced materials was very expensive because of the preparation process and other factors. They may not be used for the practical production. Then, people also found some biomass materials, such as kenaf [3,7], ramie, flax [8], hemp [9], and cotton fibers [10] for polymer composite applications, has many advantages both technically and economically. These bio-based composites enhance mechanical strength and acoustic performance, possess less weight, lower production cost, their auto interior parts are biodegradable, but currently using natural fibers is limited because of the poor actual friction and wear performance.

Recent studies indicate that the micrometric silicate mineral powders exhibit good thermal stabilities and excellent friction properties [11–13]. Dadkar et al. [11] added fly ash to reinforce phenolic based hybrid polymer matrix composites. The authors found that an increase in fly ash content decreased the degree of fade and conversely increased the frictional fluctuations (μ_{max}–μ_{min}). Cho et al. [12] prepared friction materials for brake linings using a variety of zircon particles, with diameters ranging from 1 to 150 μm. The authors found that the coarse zircon particles generated stable friction films on the lining surfaces, providing excellent frictional stability with less lining wear. Ma et al. [13] studied the effects of $ZrSiO_4$ as an abrasive in non-metallic brake friction materials. The results indicated that the $ZrSiO_4$ enhanced the friction coefficient, but depressed the wear rate. These studies demonstrate that the natural silicate minerals powders may be a potential candidate for brake friction materials components. However, there are some similar minerals, also exhibiting beneficial tribological properties, yet not to be developed. Blast furnace slag is one such example.

Table 1
The constituent ratios (wt.%) of the samples.

Raw materials	Ref.	S_1	S_2	S_3	S_4
Binders	12	12	12	12	12
Reinforced fibers[a]	21	21	21	21	21
Graphite	10	10	10	10	10
Antimony sulfide	5	5	5	5	5
Coke	9	9	9	9	9
Reinforcing fillers	43	30	20	10	0
Blast furnace slag	0	13	23	33	43

[a] Reinforcing fillers include $CaCO_3$, Al_2O_3, Feldspar powder, pure iron ore and chromite.

By-products of cast iron include the inorganic residues left behind during the cast iron melt process, called slag [14]. For steel-making plants, disposal of this slag is an environmental and economic liability, especially as changing environmental regulations have to be adhered to and disposal costs paid. In China, approximately 60% of the total amount of blast furnace slag is used beneficially as mortars, inorganic dopants, waste water disposals, fertilizers and road underlays etc. The volcanic ash activity of blast furnace slag has been extensively studied and plenty of useful information can be found [15–17]. There have, however, been few attempts to research the tribological properties of blast furnace slag in composites.

As an industrial solid waste, blast furnace slag is readily available at a negligible cost. If blast furnace slags could be used as a raw material for braking lining, it would be a considerable economic and social benefit. By analysis of its chemical constituents, we know that, blast furnace slag contains substantial amounts of silica, alumina, calcium and magnesium [16]. Those elements commonly used in current commercial brake linings. This is a strong indication that blast furnace slag has the potential to be a main ingredient in friction materials.

Blast furnace slag is typically generated at very high temperatures (N~1400 °C) [14]. This means that it could potentially provide a thermally stable bulk for high-temperature environments that a friction composite experiences. Furthermore, the specific heat capacity of blast furnace slag is relatively high (~ 0.92 J g^{-1} K^{-1}), two times to that of iron (~0.46 J g^{-1} K^{-1}). This attribute means that slag has the ability to store excess heat generated at the interfaces between brake linings and cast iron disk, thereby delaying brake linings failure under high temperatures.

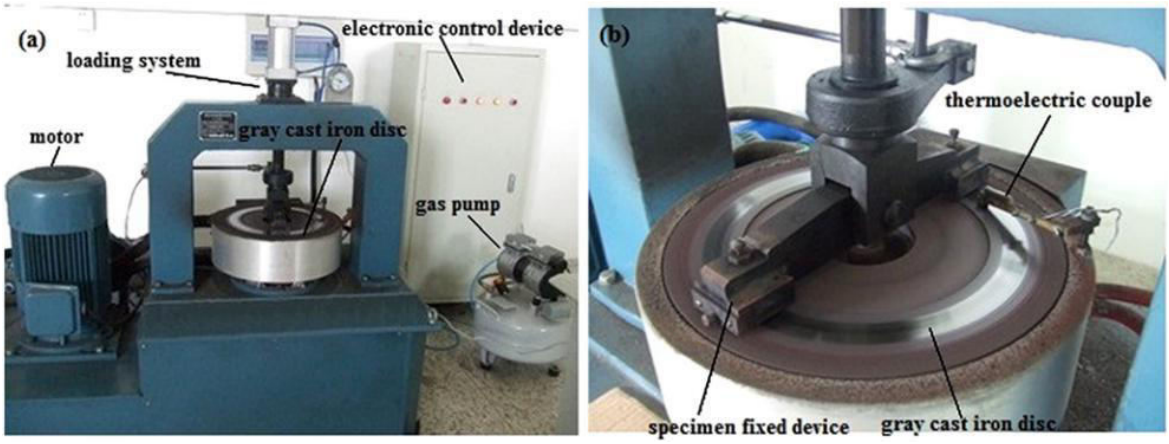

Fig. 1. (a) Experimental set-up: regulating speed friction tester: (b) 1: specimen fixed device; 2: gray cast iron disk; 3: thermoelectric couple.

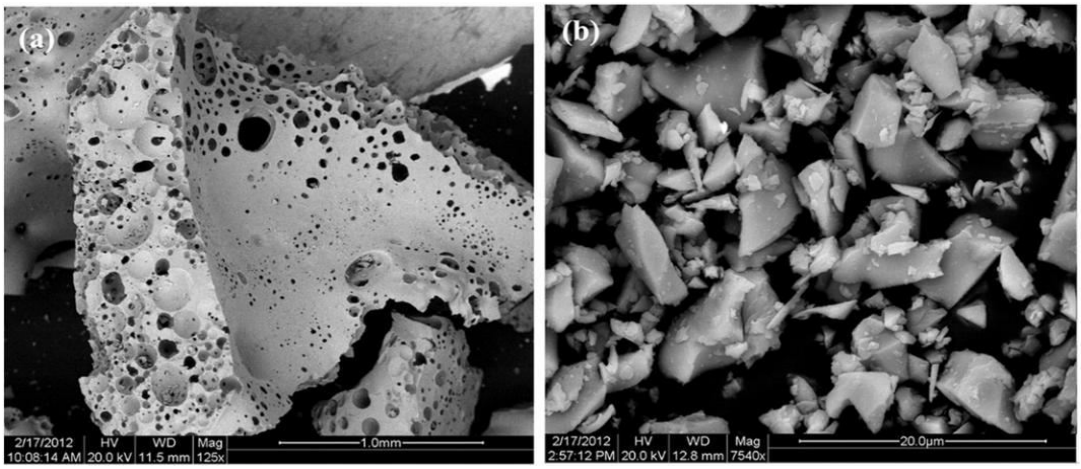

Fig. 2. Blast furnace slag: (a) original; (b) ball-grinded.

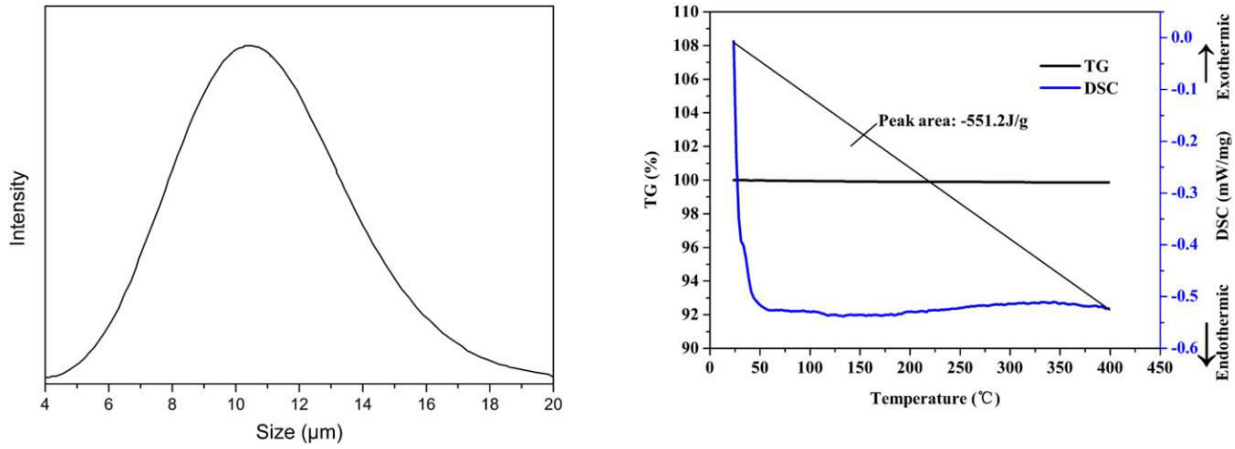

Fig. 3. Particle size distribution of blast furnace slag and TG–DSC curve of blast furnace slag under different temperatures.

The objective of this study was to investigate the properties of friction materials doped with varying amounts of high specific heat capacity blast furnace slag. Braking performances were evaluated in terms of stability of friction coefficients and wear resistances. The physico-thermal behavior of the slag particles and friction materials were also investigated by thermal analysis. Furthermore, the physical and mechanical properties were studied in order to comprehensively evaluate each set of experimental conditions. The optimal experimental conditions were chosen by comparing the properties of different brake pads, using an original, commercial automobile brake lining as a reference. The characteristics of the worn surfaces of different brake pads were studied to look at the relationship between each set of experimental conditions and performance, in an attempt to develop optimal durable friction materials with enhanced fade-recovery performance and promising wear reduction, for automotive braking applications.

2. Experimental

2.1. Raw materials

A mixture of copper fibers, steel fibers, aramid fibers and cellulose fibers (Jiangsu Veectory Group Co., Ltd., Yancheng, China) was used as reinforcements. Graphite, antimony sulfide, coke, barium sulfate, potassium feldspar, chromium iron mine and various other particles were used as space and balance fillers. Phenolic resin and NBR rubber powder (Shandong Gaoshike Industry and Trade Co., Ltd., Shandong, China) were used as binders. Blast furnace slag particles (Yancheng Lianxin Iron & Steel Co. Ltd., Jiangsu, China) were used as friction material fillers, substituting the other fillers (the weight proportion of the other fillers remain unchanged) by increasing friction in the original commercial automobile brake pad, which was kept as a reference (denoted as 'ref.'). The compositions of five friction materials were listed in Table 1. The original blast furnace slag particles were also ground for 40 min using and ball miller (diameter 500 × 500 mm).

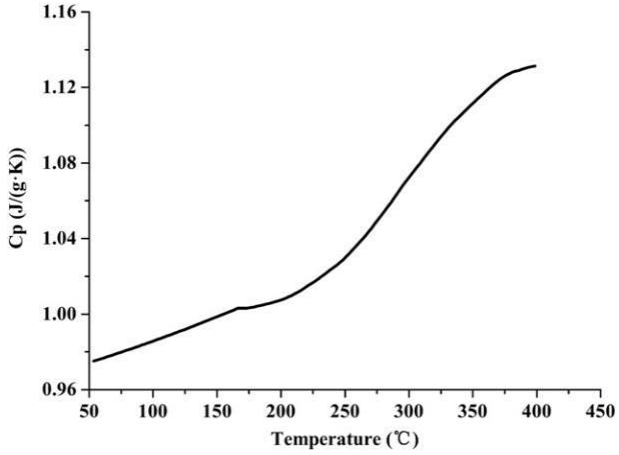

Fig. 4. Cp curve of blast furnace slag under different temperatures.

2.2. Sample preparation

The raw materials were weighed, according to the proportions given in Table 1, and then mixed, using a ball miller. The blended mixtures were put into a mold and preheated for 4 min at 160 °C. These preforms were then cured for 2 min at 160 °C, under a pressure of 40 MPa. During this process, one breathing was given at the end of each minute, preformed to release moisture and the gaseous byproducts of the cross-linking reactions (polycondensation) of the phenolic resins [2], and used to prevent composite swelling. After this, preforms were heated at 160 °C for 6 min, again under a pressure of 40 MPa. Samples were cooled down to room temperature and subsequently cured again, at 180 °C for 8 h, to relieve any frozen-in stresses. All samples were then

polished, under identical conditions, to produce uniform and maximum contact areas for tribological performance tests. Finally, the samples were characterized, looking at various physical, thermal, mechanical and tribological properties.

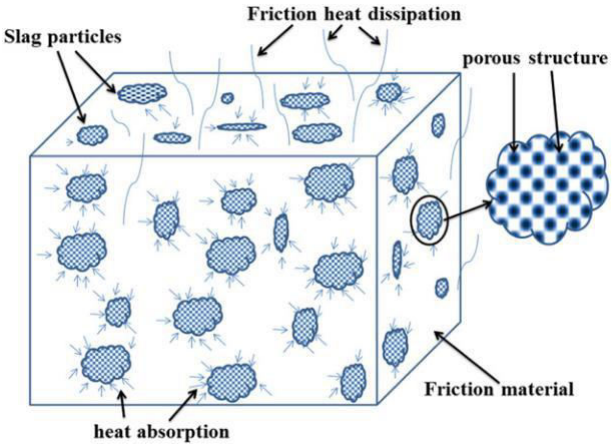

Fig. 6. Model of heat absorption of slag in the friction material

Table 2
The compositions of blast furnace slag.

Chemical composition	wt.%
CaO	35.07
SiO_2	28.73
Al_2O_3	19.82
MgO	12.58
Fe_2O_3	1.18
SO_3	1.14
TiO_2	0.83
Na_2O	0.43
P_2O_5	0.02
Others	0.20

2.3. Characterizations

Density was determined using a hydrostatic balance (Shanghai Liangping Instrument Co., Ltd.) according to the China National Standard JC/T 685-2009. Hardness was measured using a plastic Rockwell hard-ness instrument (XHR-150, Shanghai Material Tester Co., Ltd.) according to the China National Standard JJG 884-1994. Impact strength was measured using an impact tester (XJJ-5, Chengde Tester Co.,

Ltd.) and deter-mined using the method described by the China National Standard GB 5765-86. In order to ensure good data accuracy and repeatability, all tests above were repeated five times at least. SEM (QUANTA 200, FEI Co., Ltd.) was also used to examine the morphology of the slag and worn surfaces to investigate the relationship between structure and performance. Particle size distribution was conducted using a particle size analyzer (Mastersizer 3000, Malvern Instruments Ltd.).

Asynchronous thermal analyzer (STA 449C, NETZSCH Inc.) was employed to analyze thermo-gravimetric (TG), differential scanning calorimetry (DSC) and specific heat capacity (Cp), with an atmosphere simulating air. A temperature range from room temperature to 400 °C, with 10 °C min^{-1} increments, was used. Sample powder masses were 10 mg.

Tribological tests were carried out using a regulating speed friction tester (X-DM, Xianyang Xinyi Friction Sealing Equipment Co., Ltd.), shown schematically in Fig. 1a. The test rig was made up of five parts: loading system, gray cast iron disk, motor, gas pump and electronic control device. During testing, samples were fixed in place using the device shown in Fig. 1b. Prior to testing, all sample surfaces were polished. The gray cast iron disk was also cleaned with absolute alcohol. The friction material samples were tested with the gray cast iron disk as a counter-part, using a constant speed of 480 rpm and a 0.98 MPa load. The frictional force was continuously recorded at 50 °C intervals between 100 and 350 °C. An electric heater and water cooler were used to regulate testing temperatures. Temperatures were measured using a thermo-electric couple (Fig. 1b).

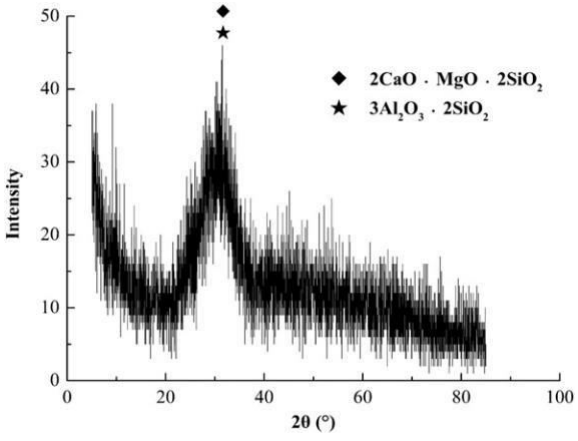

Fig. 7. XRD spectrum of blast furnace slag.

3. Results and discussions

3.1. Blast furnace slag properties and characteristics

The morphologies of the original and ball milled blast furnace slag were investigated by SEM. A large number of differently sized pores were observed in the original blast furnace slag bulk (Fig. 2a), explained by the fact that is formed after water quench at very high temperatures. Under these conditions, it is difficult to quickly release air bubbles from inside the molten slag during the sudden cooling process. That means a porous structure can be easily formed in blast furnace slag. Simultaneously, the molten slag does not have enough time to crystallize. Finally, a kind of glassy material with pore structure is formed, called original blast furnace slag. But the original blast furnace slag is with bigger pore and cannot serve for a modifier of friction materials because of the limit of the low intensity and structural defects. So the slag with a finer granularity was prepared by mechanically crushing and ball-grinding the original blast furnace slag at room temperature, for 40 min. These powders exhibited irregular shapes, with sizes b~20 μm, as can be seen in the SEM micrographs (Fig. 2b). The particle size distribution of these powders can also be shown in Fig. 3. As we know, the less particle size the powders have, the higher surface energy they have. In order to reach a steady energy state, the powders must release their energy by other ways. For example, they may attract each other. In this sense, the ball milled blast furnace slag powders may have better interface combination status between slag and other constituents in friction materials. It may also achieve good mechanical strength and tribological properties.

The ball milled blast furnace slag also should have the similar micro-structure with the original blast furnace slag, but contains only some micro ore. They would introduce some different sized micro ore into friction materials when they are added as a modifier. It is believed that the micro ore structure of the friction materials could help to absorb brake noise to reduce overall noise pollution. Furthermore, the micro ore structure can also store a considerable amount of heat during the braking process of the brake pad. This characteristic is also associated with the high specific heat capacity (C_p) of the blast furnace slag. The C_p value shows the ability to absorb (or release) heat of unit mass of a substance by unit temperature interval under specified conditions, such as constant pressure. It means heat absorption occurs when the C_p value is positive, otherwise negative values represent the heat re-lease. The C_p curve of the slag can be seen from the Fig. 4. The C_p value gradually increases from 0.97 to 1.13 J $(g\ K)^{-1}$ with an increase in temperature from 50 to 400 °C. The specific heat capacity is quite high, a potential attribute advantageous for friction modifiers. That means the slag has the ability to absorb a lot of heat. In order to further prove the process of heat absorption, TG–DSC curve of the slag was also presented in Fig. 3, where the mass of the slag can be seen to be almost constant during raising temperature. The DSC curve behaves differently, dramatically decreasing from 0 to −0.5 mW/mg under 50 °C. but the heat absorption is quite obvious and sustained above 50 °C. Heat absorption capacity can be calculated by peak area method, is about 551.2 J/g from room temperature to 400 °C. It is important evidence to confirm that the slag can absorb a very large amount of heat during the whole heating process. But for friction materials, the

thermal fade and severe wear are mainly caused by thermal decomposition of organic matter, such as resin pyrolysis. Resin often cannot withstand the higher temperature and lose the binding ability, and then the friction material would suffer the structure collapse and strength reduction when friction hap-pens. Finally, low friction coefficient and high wear rate are not expected. If the slag is as a modifier of friction material, slag can help absorb the excess heat as shown schematically in Fig. 6 and effectively prevent the thermal fade of friction and wear properties of friction material when the temperature increasing occurs.

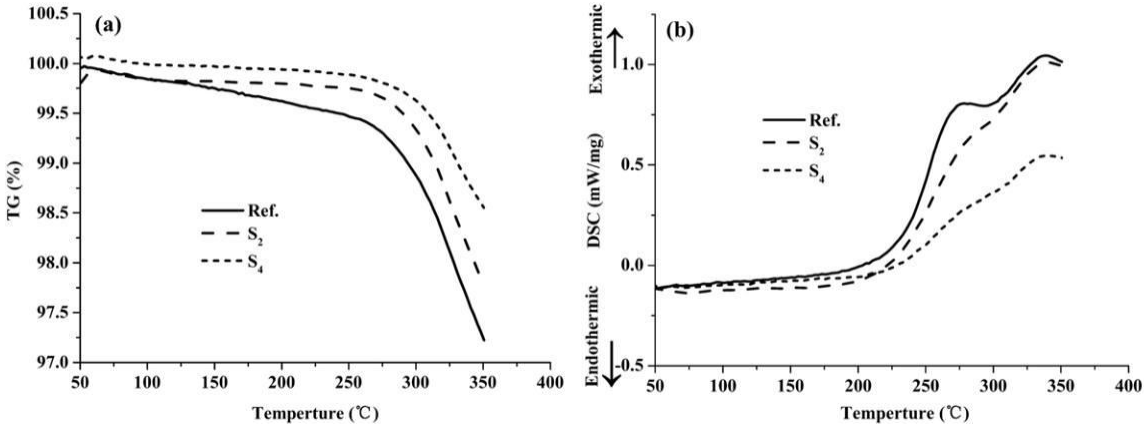

Fig. 8. TG–DSC curves of the samples with different blast furnace slag content: (a) TG; (b) DSC.

The chemical compositions of the blast furnace slag were also analyzed using an X-ray fluorescence spectrometer (ADVANT'XP, ARL Co., Ltd.) and they are listed in Table 2. By analyzing these data, the blast furnace slag can be seen to predominantly consist of calcium, silica, alumina and magnesium. The elements are also the main elemental composition of the friction materials. Therefore, the blast furnace slag is an appropriate modifier according the elemental composition. More-over, the XRD spectrum of slag is shown in Fig. 7, these elements in the form of Akermanite ($2CaO{\cdot}MgO{\cdot}2SiO_2$) and mullite ($3Al_2O_3{\cdot}2SiO_2$) match the XRF test results. No major crystalline structures or phases were observed in XRD spectra, strongly suggesting that the slag particles are amorphous. That is consistent with the glassy state structure of the slag mentioned in the previous paragraph.

3.2. Physico-thermal characterizations of frictional materials

In order to understand the influence of the slags weight fraction on the thermal stability of the friction materials, TG–DSC analyses of Ref., S_2 and S_4 were carried out, with the results shown in Fig. 8a and b. The TG curve shows mass loss during heating (50–350 °C). The figure shows that the Ref. sample have higher mass-loss rate (~2.78%), with mass-loss decreasing from ~ 2.15% to ~ 1.45% with an increase in slag doping content from 23 wt.% to 43 wt.% (for S_2 and S_4 respectively). This corresponds to a considerable weight reduction beginning at a temperature of 150 °C and continuing up to a temperature of 350 °C. This dramatic weight reduction occurs after the temperature of 250 °C, shown in Fig. 8a, can be attributed to the thermal decomposition of organic binders [2] and the oxidation of graphite.

The variations of DSC curves of the three friction materials are al-most non-existent at temperatures between 50 and 200 °C. Obvious transitions are, however, all exothermic between temperatures of 200 and 350 °C, with the chemical transformations all in terms of volatiles escaping the bulk of the friction materials. Those volatile materials are detrimental to friction materials, and they may lead a structure collapse and a failure of friction and wear properties. The main origin of the exothermic phenomena is thought to be resin degradation by oxidation of volatile elements [2,18]. Less heat release was also found from the fric-tion pads S_4 than S_2 and Ref. Because S_4 with more slag (40 wt.%) is able to effectively absorb more frictional heat, thereby reducing the possibility of brake failure. In other words, the increase of thermal stability for the polymer based friction materials is a consequence of adding slag with high specific heat capacity.

Table 3
Physical and mechanical properties of the friction materials.

Sample	Ref.	S_1	S_2	S_3	S_4
Hardness (HRL)	63.6	57.8	57.4	57.2	57.0
Density (g/cm^3)	2.354	2.292	2.324	2.330	2.351
Impact strength (kJ/m^2)	3.59	3.60	3.62	3.67	3.70

3.3. Physical and mechanical properties of friction materials

The physical and mechanical properties of the different friction materials (including unmodified and modified) are presented in Table 3. The modified materials (S_1, S_2, S_3, and S_4), prepared by replacing some of the hard filler in the parent materials, exhibited lower hardness and density than those of the parent material (Ref.). That reason is that the blast furnace slag particles were with the special porous structure. Generally, friction materials with higher hardness are not guaranteed to exhibit first-rate tribological properties as they often have stiff pedal feels and higher noise propensities [19].

As the content of blast furnace slag increased from 0 to 43 wt.%, hardness of the friction materials decreased from 63.6 HRL to 57 HRL. It may be able to make an increase of toughness of the friction materials. However, the changing trend of density is opposite to that of the hard-ness. Density of S_4 is 2.351 g/cm^3, which is much higher than S_1 of 2.292 g/cm^3. The changes in density may be ascribed to the interior voids of friction materials being filled with blast furnace slag particles.

Impact strength tends to be used to evaluate the impact resistance of a material and to estimate, to a limited extent, brittleness and tough-ness. It depends predominantly on the hardness of the filler and a combination of filler–matrix interfacial conditions. In this study, as shown in Table 3, impact strength gradually increased from 3.59 kJ/m^2 to 3.70 kJ/m^2 when the content of slag increased from 0 to 43 wt.%. This is likely to be because the toughness of the friction materials increased. In addition, when blast furnace slag particles are uniformly distributed in the continuous and stiff phenolic resin matrix, so-called “organic–in-organic complex” formed. Blast furnace slag particles may therefore act as stress concentration centers. Tiny cracks may form around the particles when outer impact stresses are imposed. The spread of these tiny cracks may also consume fracture energy [20], thereby delaying failure. Furthermore, blast furnace slag particles may also obstruct fracture formation and avoiding cracks from appearing, this is another important reason for the improvement of impact strength.

3.4. Friction and wear properties of friction materials

Five friction materials were subjected to friction and wear tests. The evolution of the friction coefficient and wear rate compared, as functions of temperature, for the loads of 0.98 MPa and the speed of 480 rpm. The tests were the same as the method used by Matějka et al. [6] and Wang et al. [21]. They showed that the method was generally used for quick assessment of friction materials by conducting a standard method according to the Chinese National Standard GB 5763-2008. It can be seen from Fig. 9 that the Ref. samples showed the worst tribological properties, with the lowest friction coefficients (0.17–0.29) and the highest wear rates during these tests.

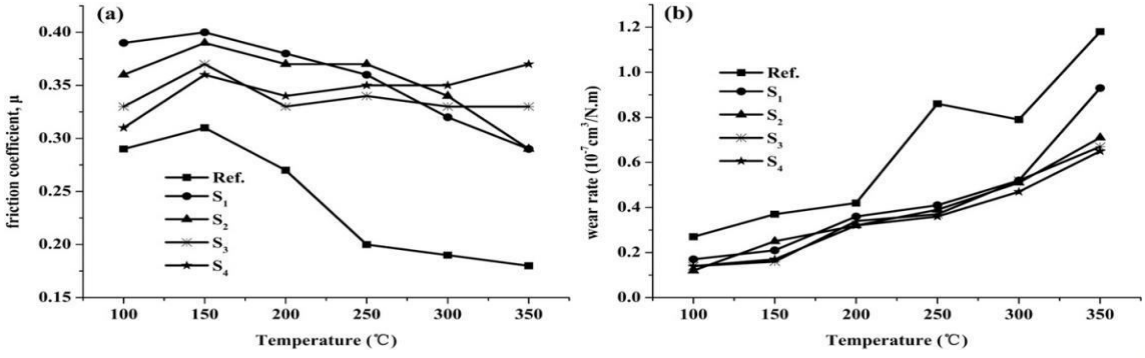

Fig. 9. Relationship between tribological performance and friction temperature: (a) friction coefficient; (b) wear rate.

The friction coefficients sharply drop from 0.31 to 0.18 significantly above 150 °C, showing noticeably fade at high temperature. But the friction coefficients of the doped frictional materials were found to be higher than that of the un-doped sample. In general, the friction coefficient was usually influenced by many factors, including frictional temperature [22], the com-positions of the counterparts [23–25], loading force [26–27] and the speed of the rotation. The loading force and the speed were constant in the tests. The effects of the temperature and compositions can't be ignored. As seen from Fig. 9a, the temperature and compositions (slag content) had a significant effect on the friction coefficient of friction materials. The friction coefficients of the doped samples showed only a minimal decrease with an increase in slag content from 13 wt.% to 43 wt.% at temperatures below 170 °C. The opposite was observed for temperatures above 300 °C. In other words, slag can decrease friction coefficients at low temperatures and increase them at the high temperatures with the doping content increase. The sample S_4 was found to have a superior and stable friction coefficient at all friction temperatures, followed by S_3. Slight heat recession was observed for S_1 and S_2 for temperatures above 150 °C. It is interesting to note here that the frictional materials based on slag exhibit friction coefficients in the range of 0.29–0.40, consistent with those of the China National Standard GB5763-2008.

The wear resistance of the friction materials was found to be mainly related to temperature and constituents (such as resins, reinforced fibers, modifiers and fillers). The effect of slag content on wear rate is shown in Fig. 9b, where wear rate curves for all the friction materials in-crease with an increase in temperature. In particular, wear rate of the Ref. is higher than the others obviously. All the slag-modified friction materials can be seen to exhibit lower wear rates. Especially, the wear rate of the Ref. is 1.18×10^{-7} $cm^3/N{\cdot}m$ at 350 °C, while slag 13%, slag 23%, slag 33%, and slag 43%, is 0.93×10^{-7} $cm^3/N{\cdot}m$, 0.72×10^{-7} $cm^3/N{\cdot}m$, 0.67×10^{-7} $cm^3/N{\cdot}m$ and 0.65×10^{-7} $cm^3/N{\cdot}m$, respectively. This is because the slag is thought to contribute to the heat absorption, since they have very high specific heat capacities. They can reduce the frictional interface temperature and decrease the thermal wear of friction materials. On the other hand, the transfer layer formed on the worn surfaces may also reduce wear.

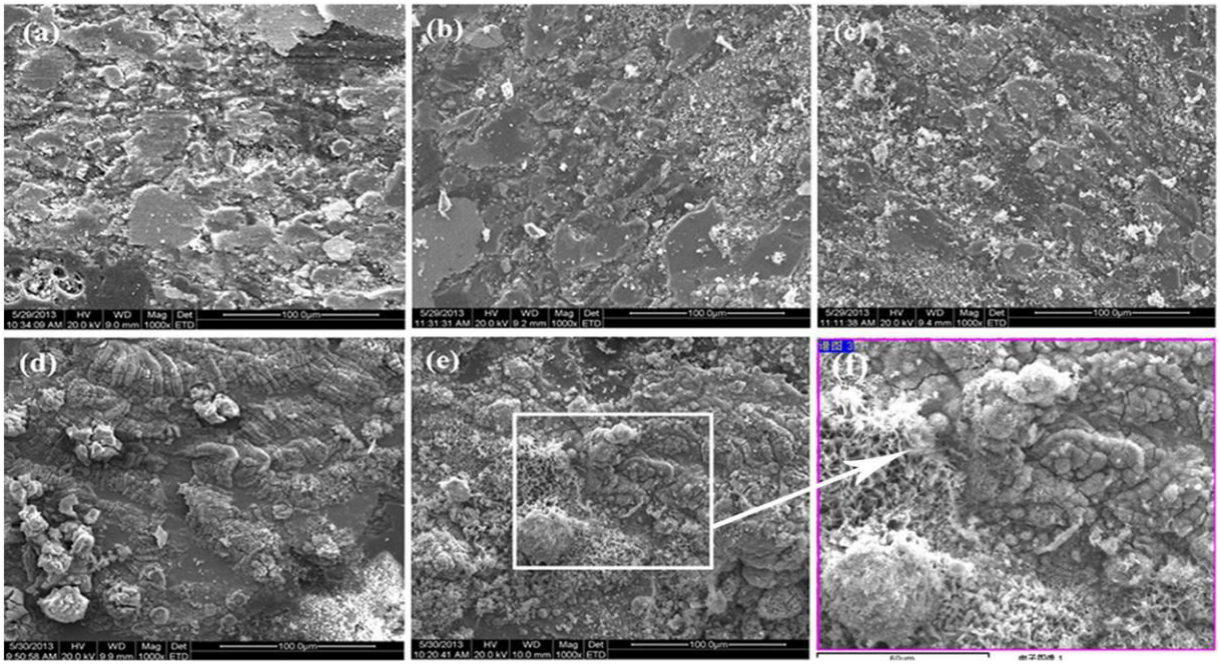

Fig. 10. SEM images of the worn surfaces of five friction materials tested under dry conditions.

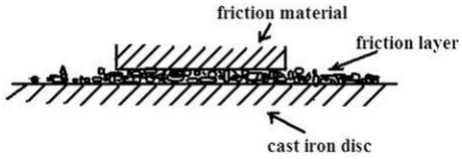

Fig. 11. The friction layer between the friction material and cast iron disk.

3.5. SEM characteristics and wear analysis

Fig. 10 shows SEM micrographs of the worn surfaces of five friction materials tested under dry sliding friction conditions. Examining the figures, some scratches and small pores are observed on the surfaces of Ref. (Fig. 10a). The wear mechanism is thought to be predominantly ploughing and adhesive wear, caused by filler–matrix debonding during the wear testing. With an increase in slag content from 13 to 23 wt.%, some wear debris is generated, acting as third body particles on the surfaces of the friction materials (Fig. 10b–c). The presence of wear debris on the worn surface reveals that, during sliding, wear particles get accumulated on the worn surface itself. Most of wear debris play an abrasive role, scratching and damaging the friction surface. They appear on the surface to be responsible for the high wear rate [21,28]. This means that the dominant wear mechanism is abrasive wear. Lots of wear debris are gradually pulverized and then fill the pits on the surfaces. In particular, the continuous and thick transfer layers are formed on the surface of friction materials S_3 and S_4 (Fig. 10d–e). The amount of transfer layers was seen to increase with an introduction of slag content. The presence of this transfer layers indicate that material transfer has occurred between the specimen surface and its counterpart (Fig. 11). These layers are thought to be formed from wear particulates generated during friction. The formation of transfer layers and the wear debris is an alternate and dynamic process. Such dynamic behavior in resin-based friction material has also been reported by Kchaou et al. [29] who have shown that the entrapped wear particles agglomerate at the interface that separates the sliding surfaces. The deposit grows larger until it reaches a critical size beyond which it collapses and new agglomerate is formed. Especially, the agglomerate is compressed into sheet when friction appears. It is so-called transfer layer. The transfer layers formed cover the friction surface and exhibit good lubrication, thereby diminishing the abrasive effect [30–31]. EDS analysis (Fig. 10f and Fig. 12) showed that morphology and composition of the transfer layer of the sample S_4, the composition consists of carbon, oxygen, magnesium, aluminum, silicium, calcium, iron and so on. Most of elements come from the blast furnace slags. It is obvious that the slag plays a role to resist thermal fade. On the other hand, silicon and aluminum typically act as abrasive elements, scratching off the cast iron disk counter face and the friction materials adhering to it. The oxygen and iron detected in the friction layer are very likely to be in the form of iron oxide particles, coming from the cast iron brake disk. The presence of iron oxide is another indicator of good heat dissipation at the friction interface. The analysis in this study clearly indicates slag can help form the transfer layers on the brake surface that is responsible for the overall performance changes.

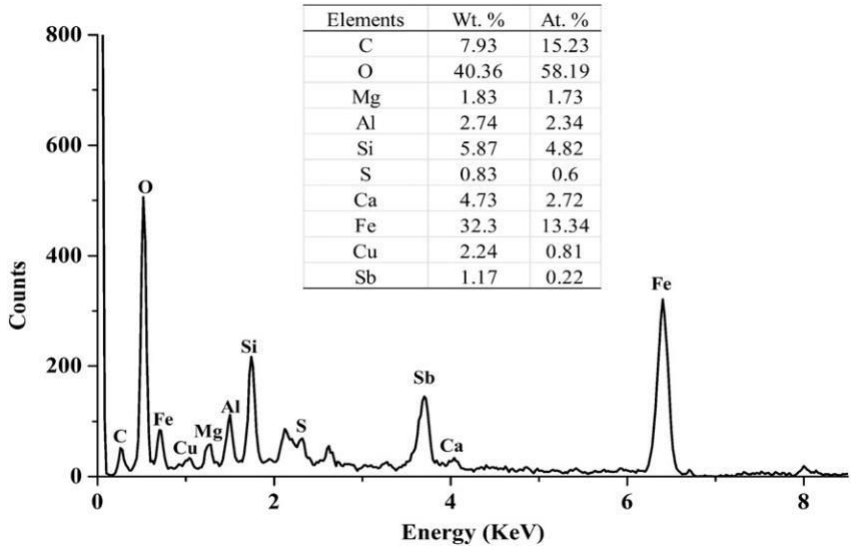

Fig. 12. EDS of the worn surface of sample S_4.

4. Conclusions

(1) There are a lot of differently sized pores in the original blast furnace slag bulk; the ball milled blast furnace slag powders exhibited irregular shapes (with sizes b~ 20 μm), amorphous structures, high Specific heat capacity (0.97–1.13 J (g K)$^{-1}$ from 50 to 400 °C).

(2) The Ref. sample have higher mass-loss rate (~2.78%). The mass-loss decrease from ~ 2.15% to ~ 1.45% when an increase in slag doping content from 23 wt.% to 43 wt.%.

(3) DSC curves of friction materials are similar at temperatures be-tween 50 and 200 °C. Less heat release was found for the friction pads S_4 than S_2 and Ref. between temperatures of 200 and 350 °C.

(4) The modified materials exhibited lower hardness and density than the Ref. Hardness of the friction materials decreased from 63.6 HRL to 57.0 HRL as the content increased from 0 to 43 wt.%, but density is opposite. Density of S_4 (2.351 g/cm^3) is much higher than others. Impact strength gradually increases from 3.59 kJ/m^2 to 3.70 kJ/m^2 when the content of slag increases from 0 to 43 wt.%.

(5) The Ref. samples showed the lowest friction coefficients (0.17– 0.29) and the highest wear rates (1.18×10^{-7} cm^3/N·m at 350 °C) during these tests. The wear mechanism is mainly ploughing and adhesive wear. For the doped samples, the friction coefficients show only a minimal decrease with slag con-tent increase from 13 wt.% to 43 wt.% at temperatures below 170 °C. The opposite was observed for temperatures above 300 °C. The sample S_4 has a more superior and stable friction coefficient than others because of the transfer layers formed on the surface of friction materials.

On the basis of conclusions above, the more details will be done. The effects of the slag on the tribological behavior of friction materials with the different temperatures/loads/speeds will be studied further subsequently. In the future, the more modified slags will be probably exploited and developed for the friction materials with higher performance. The high-value research will also be considered related to the tribological properties of slags.

Acknowledgments

This research is supported by a Youth Fund of National Natural Science Foundation of PR China (21301149), Natural Science Research Pro-gram of Jiangsu (BK20141262), A Project Funded by the Priority Academic Program Development of Jiangsu Higher Education Institutions and the Opening Project of Laboratory of Yancheng Institute of Technology. The authors also acknowledge Dr. Jingwen Chen in the preparation of manuscript.

References

[1] R. Hinrichs, M.R.F. Soares, R.G. Lamb, et al., Phase characterization of debris generated in brake pad coefficient of friction tests, Wear 270 (2011) 515–519.

[2] R. Ertan, N. Yavuz, An experimental study on the effects of manufacturing parameters on the tribological properties of brake lining materials, Wear 268 (2010) 1524–1532.

[3] A. Mustafa, M.F.B. Abdollah, F.F. Shuhimi, et al., Selection and verification of kenaf fibres as an alternative friction material using Weighted Decision Matrix method, Mater. Des. 67 (2015) 577–582.

[4] J. Fei, H.K. Wang, J.F. Huang, et al., Effects of carbon fiber length on the tribological properties of paper-based friction materials, Tribol. Int. 72 (2014) 179–186.

[5] Q.H. Wang, X.R. Zhang, X.Q. Pei, Study on the friction and wear behavior of basalt fabric composites filled with graphite and nano-SiO_2, Mater. Des. 31 (2010) 1403–1409.

[6] V. Matějka, Y.F. Lu, L. Jiao, et al., Effects of silicon carbide particle sizes on friction-wear properties of friction composites designed for car brake lining applications, Tribol. Int. 43 (2010) 144–151.

[7] Y.A. El-Shekeil, S.M. Sapuan, K. Abdan, et al., Influence of fiber content on the mechanical and thermal properties of kenaf fiber reinforced thermoplastic polyurethane composites, Mater. Des. 40 (2012) 299–303.

[8] Z.Z. Fu, B.T. Suo, R.P. Yun, et al., Development of eco-friendly brake friction compos-ites containing flax fibers, J. Reinf. Plast. Compos. 31 (10) (2012) 681–689.

[9] V. Placet, Characterization of the thermo-mechanical behaviour of hemp fibres intended for the manufacturing of high performance composites, Compos. Part A 40 (2009) 1111–1118.

[10] M. Uzun, K.K. Govarthanam, S. Rajendran, Interaction of a non-aqueous solvent sys-tem on bamboo, cotton, polyester and their blends: the effect on abrasive wear resistance, Wear 322-323 (2015) 10–16.

[11] N. Dadkar, B.S. Tomar, B.K. Satapathy, Evaluation of fly ash-filled and aramid fibre reinforced hybrid polymer matrix composites (PMC) for friction braking applications, Mater. Des. 30 (2009) 4369–4376.

[12] K.H. Cho, H. Jang, Y.S. Hong, et al., The size effect of zircon particles on the friction

characteristics of brake lining materials, Wear 264 (2008) 291–297.

[13] Y.N. Ma, G.S. Martynková, M. Marta Valáškováb, et al., Effects of $ZrSiO_4$ in non-metallic brake friction materials on friction performance, Tribol. Int. 41 (2008) 166–174.

[14] A. Lotfy, K.M.A. Hossain, M. Lachemi, et al., Statistical models for the development of optimized furnace slag lightweight aggregate self-consolidating concrete, Cement & Concrete Composites 55 (2015) 169–185.

[15] H.A. Razak, F. Sajedi, The effect of heat treatment on the compressive strength of cement-slag mortars, Mater. Des. 32 (2011) 4618–4628.

[16] F. Sajedi, H.A. Razak, Effects of thermal and mechanical activation methods on compressive strength of ordinary Portland cement-slag mortar, Mater. Des. 32 (2011) 984–995.

[17] P. Dinakar, K.P. Sethy, U.C. Sahoo, Design of self-compacting concrete with ground granulated blast furnace slag, Mater. Des. 43 (2013) 161–169.

[18] M. Kumar, B.K. Satapathy, A. Patnaik, et al., Hybrid composite friction materials rein-forced with combination of potassium titanate whiskers and aramid fibre: assessment of fade and recovery performance, Tribol. Int. 44 (2011) 359–367.

[19] M. Boz, A. Kurt, The effect of Al_2O_3 on the friction performance of automotive brake friction materials, Tribol. Int. 40 (2007) 1161–1169.

[20] I. Guiamatsia, G.D. Nguyen, A thermodynamics-based cohesive model for interface debonding and friction, Int. J. Solids Struct. 51 (2014) 647–659.

[21] F.H. Wang, Y. Liu, Mechanical and tribological properties of ceramic-matrix friction materials with steel fiber and mullite fiber, Mater. Des. 57 (2014) 449–455.

[22] Z.Q. Wang, D.R. Gao, Friction and wear properties of stainless steel sliding against polyetheretherketone and carbon-fiber-reinforced polyetheretherketone under natural seawater lubrication, Mater. Des. 53 (2014) 881–887.

[23] F. Eddoumy, H. Kasem, H. Dhieb, et al., Role of constituents of friction materials on their sliding behavior between room temperature and 400 °C, Mater. Des. 65 (2015) 179–186.

[24] J.G. Xu, H.B. Yan, D.G. Gu, Friction and wear behavior of polytetrafluoroethene composites filled with Ti_3SiC_2, Mater. Des. 61 (2014) 270–274.

[25] A. Almaslow, M.J. Ghazali, R.J. Talib, et al., Effects of epoxidized natural rubber– alumina nanoparticles (ENRAN) composites in semi-metallic brake friction mate-rials, Wear 302 (2013) 1392–1396.

[26] S.F. Zhou, Q.X. Zhang, C.Q. Wu, et al., Effect of carbon fiber reinforcement on the me-chanical and tribological properties of polyamide6/polyphenylene sulfide compos-ites, Mater. Des. 44 (2013) 493–499.

[27] S.R. Chauhan, S. Thakur, Effects of particle size, particle loading and sliding distance on the friction and wear properties of cenosphere particulate filled vinylester composites, Mater. Des. 51 (2013) 398–408.

[28] F. Findik, Latest progress on tribological properties of industrial materials, Mater. Des. 57 (2014) 218–244.

[29] M. Kchaou, A. Sellami, R. Elleuch, et al., Friction characteristics of a brake friction material under different braking conditions, Mater. Des. 52 (2013) 533–540.

[30] M.H. Cho, K.H. Cho, S.J. Kim, The role of transfer layers on friction characteristics in the sliding interface between friction materials against gray iron brake disks, Tribol. Lett. 20 (2) (2005) 101–108.

[31] P.L. Menezesa, K.K.S.V. Kishore, et al., Friction and transfer layer formation in polymer-steel

tribo-system: role of surface texture and roughness parameters, Wear 271 (2011) 2213–2221.